

ZS-TreeSeg: A Zero-Shot Framework for Tree Crown Instance Segmentation

Pengyu Chen, Fangzheng Lyu, Sicheng Wang, and Cuizhen Wang

Abstract—Individual tree crown segmentation is an important task in remote sensing for forest biomass estimation and ecological monitoring. However, accurate delineation in dense, overlapping canopies remains a bottleneck. While supervised deep learning methods suffer from high annotation costs and limited generalization, emerging foundation models (e.g., Segment Anything Model) often lack domain knowledge, leading to under-segmentation in dense clusters. To bridge this gap, we propose ZS-TreeSeg, a Zero-Shot framework that adapts from two mature tasks: 1) Canopy Semantic segmentation; and 2) Cells instance segmentation. By modeling tree crowns as star-convex objects within a topological flow field using Cellpose-SAM, the ZS-TreeSeg framework forces the mathematical separation of touching tree crown instances based on vector convergence. Experiments on the NEON and BAMFOREST datasets and visual inspection demonstrate that our framework generalizes robustly across diverse sensor types and canopy densities, which can offer a training-free solution for tree crown instance segmentation and labels generation.

Index Terms—Instance segmentation, tree crown delineation, zero-shot learning, foundation model.

I. INTRODUCTION

TREE crown instance segmentation remains a challenging problem in remote sensing due to the complex spatial structure of forest canopies [1], [2]. Unlike discrete objects in general imagery, tree crowns in dense stands exhibit overlapping branches and ambiguous visual boundaries, making the definition of individual instances inherently difficult [3].

Existing approaches to this problem face distinct methodological barriers. On one hand, supervised learning models suffer from a dependency on large-scale instance annotations. Generating such ground truth is labor-intensive and prone to subjectivity even among experts [3], [4], severely limiting model generalizability and scalability. On the other hand, recent foundation models such as the Segment Anything Model (SAM) [5] have significantly improved general-purpose segmentation. However, when applied to tree crown instance segmentation, these models often struggle in dense forests where adjacent crowns exhibit ambiguous boundaries [6]. Some studies enhance instance separability by combining other data sources, such as tree height information from LiDAR [7], Digital Surface Models (DSMs) [8], and multi-spectral features [9]. Although effective, these multi-modal

approaches often entail higher data acquisition costs and computational complexity, limiting their scalability.

To overcome these limitations without relying on expensive auxiliary data or annotations, we draw inspiration from adjacent fields. We observe that semantic segmentation of tree canopies has reached a high level of maturity [10], [11], providing reliable foreground priors. Furthermore, tree crowns share star-convex morphological properties with biological cells. In biomedical imaging, flow-based methods such as CellViT [12] and Cellpose-SAM [13] successfully separate touching instances by predicting gradient fields, a mechanism highly transferable to canopy delineation.

Building on these insights, we propose ZS-TreeSeg, a zero-shot framework that synergizes mature canopy semantic segmentation with flow-based instance delineation. By using semantic masks to constrain the search space and integrating Cellpose-style flow dynamics with SAM, our approach achieves robust instance segmentation without requiring instance-level training data.

II. METHODOLOGY

The core methodological innovation of this study is the reconceptualization of tree crown delineation as a topological flow-convergence problem rather than a traditional boundary detection task. Our approach leverages the structural isomorphism between biological cells and tree crowns, both of which are star-convex objects, to apply gradient flow dynamics for separating dense, touching instances without supervision. Crucially, we employ a semantic prior (SegFormer) to spatially regularize Cellpose-SAM, preventing background over-segmentation and enabling robust zero-shot generalization.

The workflow is illustrated in Figure 1, executes this concept in two stages: 1) Canopy Semantic Constraint, which isolates the search space to valid canopy regions; and 2) Flow-guided Instance Segmentation, which forces the separation of individual crowns. The specific implementation details are described in Sections 2A and 2B, respectively.

A. Semantic Segmentation

In the ZS-TreeSeg’s first stage, a SegFormer model (MiT-B5 backbone) trained on the OAM-TCD (OpenAerialMap-tree crown delineation) dataset [14] is used to perform binary semantic segmentation of tree canopies. The model achieves an F_1 score of 0.914 and an Intersection-over-Union (IoU) of 0.887, producing a semantic mask $M_{\text{sem}} \in \{0, 1\}^{H \times W}$ that delineates canopy pixels (class 1) from background elements (class 0), including soil, roads, and built-up areas [14].

P. Chen, S. Wang, and C. Wang are with the Department of Geography, University of South Carolina, Columbia, SC 29208 USA (e-mail: pengyuc@email.sc.edu; SICHENGW@mailbox.sc.edu; CWANG@mailbox.sc.edu).

F. Lyu is with the Department of Geography, Virginia Polytechnic Institute and State University, Blacksburg, VA 24061 USA (e-mail: fangzheng@vt.edu).

Corresponding author: Fangzheng Lyu.

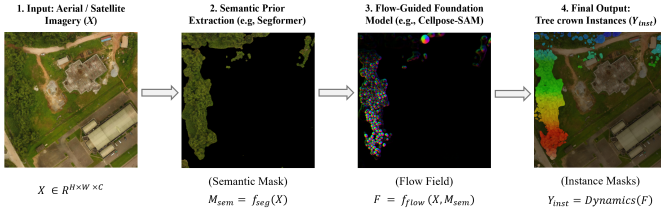


Fig. 1. Overview of the Zero-Shot Tree Crown Segmentation Framework. The pipeline integrates a semantic prior to extract the canopy mask, followed by a cell segmentation model (Cellpose-SAM) that predicts gradient vector fields to isolate individual tree instances.

This semantic mask serves as a spatial constraint for the subsequent zero-shot instance segmentation stage. Although foundation models such as SAM and Cellpose-SAM exhibit strong generalization capabilities, their predictions remain sensitive to background textures in high-resolution aerial imagery [6]. In particular, Cellpose-SAM was derived from SAM and further fine-tuned using large-scale cellular imagery [13], which tends to generate spurious instance detections in visually complex non-canopy regions when applied without prior spatial filtering.

As shown in Fig. 2, omitting semantic filtering results in pronounced over-segmentation over background surfaces such as grass and rooftops. By contrast, applying the semantic prior M_{sem} effectively restricts instance inference to canopy regions, substantially reducing false positives and improving the stability of zero-shot predictions.

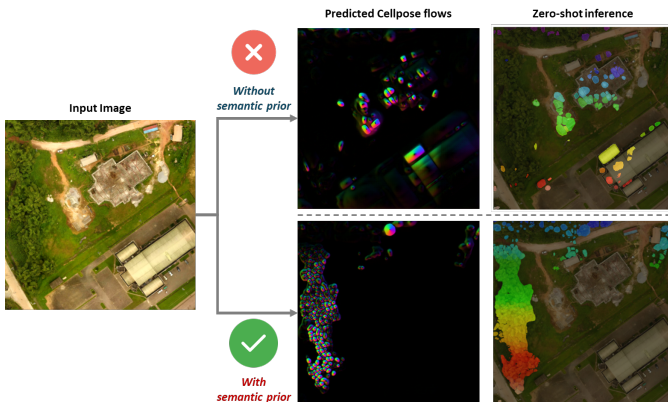


Fig. 2. Effect of semantic masking on zero-shot instance segmentation. (Top) Results without semantic filtering, showing erroneous detections over background textures. (Bottom) Results with semantic prior (M_{sem}), where instance predictions are constrained to canopy regions.

Semantic segmentation is treated as a preprocessing step rather than a core contribution of this work. Given the maturity of canopy segmentation in remote sensing and the availability of high-performing pretrained models, SegFormer is employed as an off-the-shelf component to provide a reliable region of interest (ROI) for downstream instance segmentation.

B. Flow-guided Instance Segmentation Framework

ZS-TreeSeg framework adapts the Cellpose-SAM architecture for tree-crown delineation by leveraging the geometric

property that biological cells and tree crowns share a quasi-star-convex structure [15], [16]. This inductive bias is particularly effective for separating dense, touching crowns in aerial imagery where explicit boundary cues are often ambiguous. As illustrated in Fig. 3, the segmentation process is formulated as a dynamical system involving latent feature encoding, gradient field prediction, and iterative pixel convergence.

First, to capture high-level semantic context, the input image \mathbf{I} is mapped into a shape-aware latent space using the SAM-based Vision Transformer (ViT) backbone. Unlike convolutional encoders with limited receptive fields, the ViT encoder, denoted as Φ_{ViT} , aggregates global contextual information to produce a robust feature representation \mathbf{Z} :

$$\mathbf{Z} = \Phi_{\text{ViT}}(\mathbf{I}). \quad (1)$$

This representation implicitly encodes object interior structures and spatial dependencies, providing a rich basis for distinguishing individual instances within crowded canopies.

Subsequently, the network predicts a pixel-wise vector field \mathbf{V} based on the local latent features \mathbf{Z}_p . Theoretically, this field represents the spatial gradient of an instance-specific potential surface Ψ , which exhibits local minima at object centers. The predicted flow vector at pixel p is obtained by decoding the feature representation:

$$\mathbf{V}(p) = \nabla \Psi(p) \approx \text{Decoder}(\mathbf{Z}_p), \quad (2)$$

where $\text{Decoder}(\cdot)$ denotes the prediction head mapping latent features to 2D flow vectors. Geometrically, $\mathbf{V}(p)$ guides pixels inward toward the centroid (sink) of their respective instances. By approximating this gradient field, the network naturally handles topology; the flow diverges at the boundaries between touching crowns and converges within crown interiors, effectively converting segmentation into a flow prediction task.

Finally, instance masks are recovered through a flow-convergence grouping process during inference. Pixels are treated as particles in a dynamical system and are iteratively advected along the predicted stream lines using Euler integration:

$$p_{\tau+1} = p_{\tau} + \mathbf{V}(p_{\tau}), \quad (3)$$

where τ denotes the iteration step. As $\tau \rightarrow \infty$, pixels belonging to the same crown converge to a common stable fixed point S_k . The set of all pixels whose trajectories terminate at S_k constitutes the k -th instance mask \mathcal{M}_k . This mechanism ensures robust instance separation solely through flow dynamics, eliminating the need for post-processing steps like watershed transforms or non-maximum suppression.

The complete inference workflow, detailing the sequential application of semantic masking and flow-based grouping, is presented in Algorithm 1.

III. RESULTS

This section evaluates the performance of the ZS-TreeSeg framework. The analysis is organized into three components: a qualitative assessment of the model's zero-shot generalization across varying scales and densities, a quantitative benchmark on the NEON and BAMFORESTS datasets, and a detailed visual inspection comparing the framework against supervised baselines in complex environments.

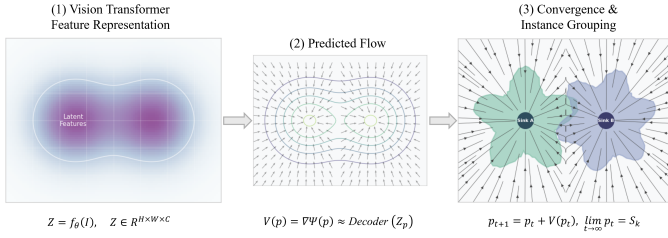


Fig. 3. Conceptual framework of the proposed flow-based segmentation. (1) Feature Encoding: A ViT backbone extracts a latent representation Z capturing global shape context. (2) Flow Prediction: The network predicts a unit vector field V (gradient of a diffusion potential) that directs pixels toward object interiors. (3) Grouping: Segmentation is achieved by iteratively tracking pixel trajectories until they converge to stable sinks.

Algorithm 1 Inference Workflow for Tree Crowns

Require: Input image X , semantic canopy mask M_{sem}

- 1: **Stage 1: Semantic masking**
 - 2: $X_{\text{masked}} \leftarrow X \odot M_{\text{sem}}$
 - 3: **Stage 2: Flow prediction**
 - 4: $(\Delta y, \Delta x, P) \leftarrow \text{CellposeSAM}(X_{\text{masked}})$
 - 5: **Stage 3: Flow-based grouping (gradient tracking)**
 - 6: // The cell probability threshold is set to 0 to avoid filtering out candidate targets
 - 7: $S \leftarrow \{\text{flow_threshold} = 1, \text{cellprob_threshold} = 0\}$
 - 8: $Y_{\text{inst}} \leftarrow \text{AdvectAndCluster}(\Delta y, \Delta x, P; S)$
 - 9: **return** Y_{inst}
-

A. Qualitative Assessment of Zero-Shot Capabilities

Our experiments demonstrate that the ZS-TreeSeg framework achieves stable accuracy and strong generalization across diverse land cover contexts without requiring any task-specific fine-tuning. As illustrated in Figure 4, the model effectively handles the multi-scale nature of forestry. It exhibits a robust capability to delineate tree crowns of varying sizes, successfully capturing both large, isolated heritage trees and smaller, clustered saplings within the same inference pass.

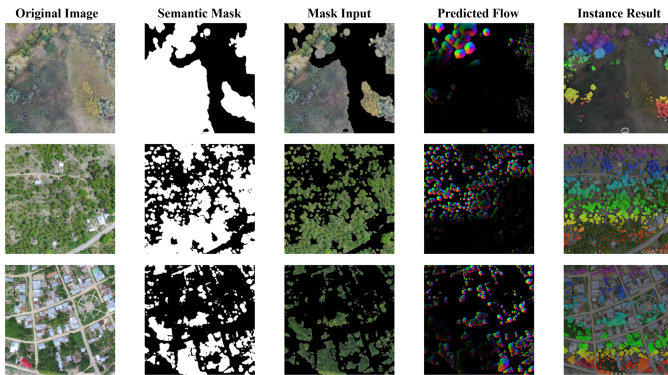


Fig. 4. Results of the zero-shot instance segmentation. The model demonstrates robust generalization across different scales and species, accurately delineating both large isolated crowns and smaller, clustered trees.

We further analyzed the model’s behavior under varying canopy densities to understand its operational boundaries. Figure 5 presents a comparative visualization between sparse urban scenarios and dense forest environments.

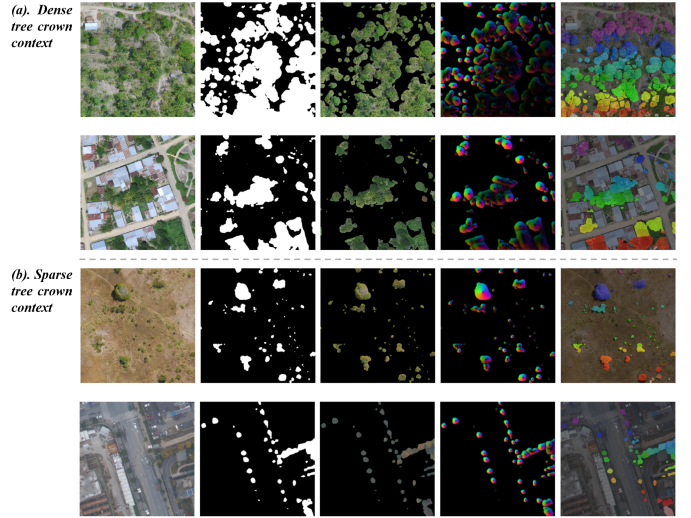


Fig. 5. Performance comparison across varying canopy densities. While the model achieves near-perfect segmentation in sparse urban contexts (top), it also maintains high separability in dense, overlapping canopy environments (bottom) by leveraging flow field dynamics.

In sparse contexts, such as street trees or suburban parks, the approach performs exceptionally well. The semantic prior effectively isolates the Region of Interest (ROI), and the distinct spatial separation between instances makes the gradient flow prediction highly reliable.

In dense contexts, where tree crowns are heavily interconnected or overlapping, the flow-guided mechanism proves critical. Unlike traditional boundary-based methods that often under-segment fused canopies, our method successfully partitions dense clusters by identifying distinct topological centroids. However, we acknowledge that in extreme cases of canopy fusion, minor over-segmentation or boundary ambiguity may persist. This suggests that while the zero-shot baseline is strong, these complex areas could still benefit from minimal manual refinement.

B. Quantitative Performance

To assess the generalizability of the ZS-TreeSeg framework, we conducted a benchmark evaluation across two diverse datasets: NEON [17] (aerial RGB) and BAMFORESTS [18] (UAV VHR). The quantitative results are summarized in Table I.

On the NEON dataset (Panel A), ZS-TreeSeg achieves an mAP@50 of 42.30%. While the supervised detection specialist DeepForest achieves higher accuracy (49.89%) due to its optimized bounding-box regression, our zero-shot segmentation approach outperforms the point-supervised TreePseCo (41.68%) [19]. This demonstrates superior capability in separating touching crowns without explicit training.

On the BAMFORESTS dataset (Panel B), which consists of VHR UAV imagery, our framework achieves an mAP@50 of 67.31%. This performance is competitive with fully supervised baselines such as Mask R-CNN (69.05%) and Mask2Former (68.89%) [20], confirming that the geometric priors leveraged by ZS-TreeSeg are transferable and effectively bridge the gap between zero-shot inference and supervised accuracy.

TABLE I
QUANTITATIVE COMPARISON ON NEON AND BAMFORESTS DATASETS.

Method	Source	Type	mAP@50 (%)
<i>Panel A: NEON Dataset (Aerial RGB)</i>			
DeepForest	[19]	Supervised (Box)	49.89
ZS-TreeSeg		Zero-Shot	42.30
TreePseCo	[19]	Supervised (Point)	41.68
<i>Panel B: BAMFORESTS Dataset (UAV VHR)</i>			
Mask R-CNN	[20]	Supervised	69.05
Mask2Former	[20]	Supervised	68.89
ZS-TreeSeg		Zero-Shot	67.31

C. Visual Inspection

To validate the efficacy of our hybrid framework beyond standard metrics, we performed a visual comparison against representative baselines. We included the TCD dataset [14] in this visual analysis. Although TCD was excluded from the quantitative benchmark due to significant granularity mismatches, where ground truth annotations frequently aggregate dense clusters into single polygons, it serves as a critical stress test for evaluating model behavior in both dense and sparse canopy environments.

The baselines exhibit failure modes on TCD’s test dataset (Figure 6). The supervised Mask R-CNN (trained on TCD) leans toward under-segmentation, frequently merging adjacent trees into single coarse clusters, reflecting the aggregation bias of its training data. Conversely, the domain-specific tool Detectree2 [21] suffers from diminished adaptability, demonstrating low precision by classifying non-tree background features as crowns. In contrast, ZS-TreeSeg achieves the optimal trade-off. The semantic prior acts as a robust filter to eliminate background noise, while the geometric flow mechanism enforces the topological separation of touching crowns. This resolves the aggregation issues common to standard supervised models, even in cases where the ground truth itself lacks fine-grained separability.

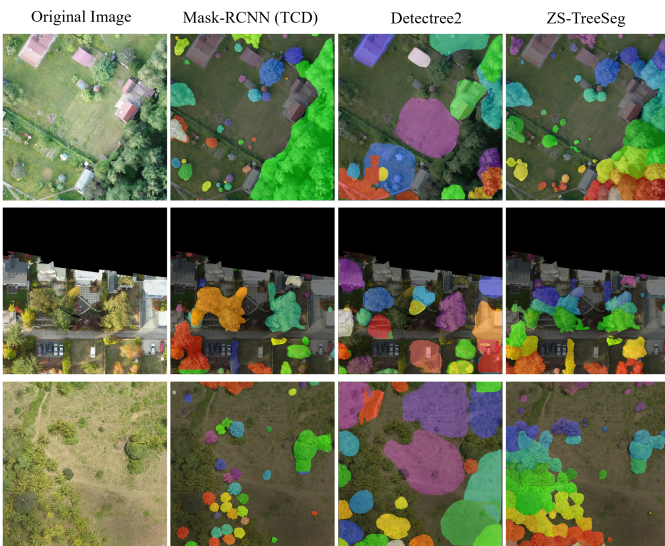


Fig. 6. Comparison with Mask R-CNN (TCD) and Detectree2.

We also visually verified the model’s domain transfer capability on the BAMFORESTS dataset (Figure 7). The resulting

segmentations demonstrate that ZS-TreeSeg reliably delineates accurate and well-defined boundaries in previously unseen domains, and does so without exhibiting the sensitivity and instability that are frequently reported for other foundation models (e.g., SAM [6]).

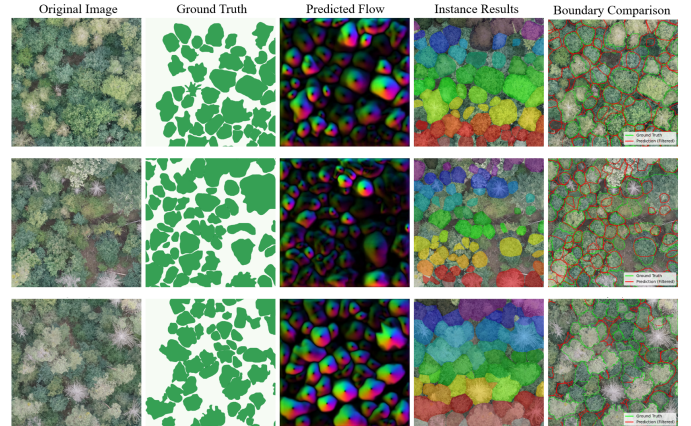


Fig. 7. Generalization test on the BAMFORESTS dataset.

IV. DISCUSSION

In this section, we discuss two key aspects observed during our evaluation: the challenges regarding dataset standardization and the practical utility of the model’s physical parameters.

A. Granularity Mismatch and Data Standardization

The qualitative discrepancy observed in the TCD evaluation points to a fundamental conflict in benchmarking: granularity mismatch. While ZS-TreeSeg enforces the topological separation of distinct tree centers, datasets like TCD frequently aggregate dense clusters into single polygons. Valid fine-grained predictions would be paradoxically penalized as false positives, rendering standard quantitative evaluation unreliable. For this reason, we excluded TCD from our quantitative benchmarks, as the ground truth ambiguity precludes a fair assessment of instance-level separability.

This limitation extends beyond a single dataset; it underscores an urgent need for the remote sensing community to develop large-scale, high-precision benchmarks that harmonize semantic richness with consistent, individual-level annotations.

By providing robust delineation, the ZS-TreeSeg framework offers a scalable way to generate high-quality ground truth and fill this gap in future datasets.

B. Diameter Sensitivity as a Physical Prior

Unlike fully opaque end-to-end deep learning models, our framework retains an explicit physical parameter: the average crown diameter. As illustrated in Figure 8, this parameter governs the convergence scale of the flow field, directly influencing how ambiguous boundaries are resolved. For instance, a smaller diameter prior encourages the separation of dense, fragmented instances (e.g., in urban settings or sapling

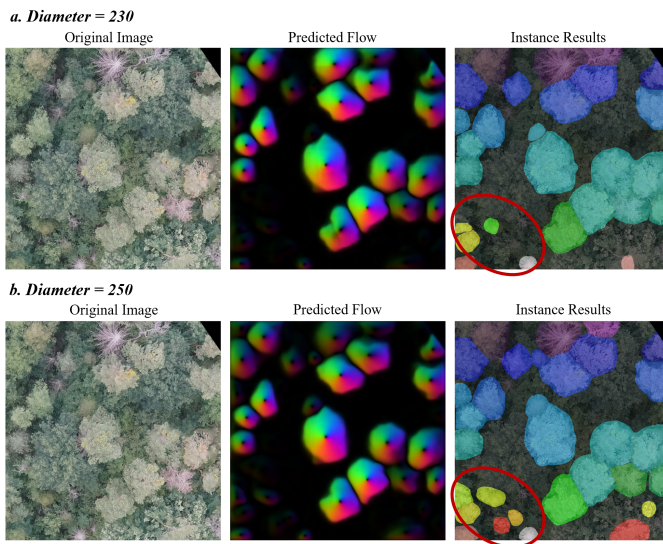


Fig. 8. The impact of the diameter prior.

stands), whereas a larger diameter promotes the aggregation of continuous canopies typical of mature forests. This sensitivity effectively allows for the injection of biological priors into the inference process. It enables foresters to tailor the segmentation granularity to specific stand ages or species characteristics without the need for computational retraining, offering a significant practical advantage for operational forest management.

V. CONCLUSION

In this letter, we present a training-free framework for individual tree crown segmentation that decouples Semantic Prior Extraction (via SegFormer) from Flow-Guided Instance Separation (via Cellpose-SAM). By leveraging geometric flow dynamics, our approach achieves robust zero-shot generalization, outperforming comparable segmentation methods on the benchmark NEON and BAMFORESTS dataset. By providing an out-of-the-box solution, this framework not only facilitates efficient large-scale forest monitoring but also offers a rapid method for generating high-quality instance mask labels to support future data annotation efforts.

REFERENCES

- [1] E. Tusa, J.-M. Monnet, J.-B. Barré, M. D. Mura, M. Dalponte, and J. Chaussoot, "Individual tree segmentation based on mean shift and crown shape model for temperate forest," *IEEE Geoscience and Remote Sensing Letters*, vol. 18, no. 12, pp. 2052–2056, 2021.
- [2] Z. Ding, H. Zhang, R. Wang, L. Zhang, H. Jiang, and T. Yun, "A dual-branch deep learning framework at the grid scale for individual tree segmentation," *IEEE Geoscience and Remote Sensing Letters*, vol. 22, pp. 1–5, 2025.
- [3] F. Lucena, F. M. Breunig, and H. Kux, "The combined use of uav-based rgb and dem images for the detection and delineation of orange tree crowns with mask r-cnn: An approach of labeling and unified framework," *Future Internet*, vol. 14, no. 10, p. 275, 2022.
- [4] B. G. Weinstein, S. Marconi, S. Bohlman, A. Zare, and E. White, "Individual tree-crown detection in rgb imagery using semi-supervised deep learning neural networks," *Remote Sensing*, vol. 11, no. 11, p. 1309, 2019.
- [5] A. Kirillov, E. Mintun, N. Ravi, H. Mao, C. Rolland, L. Gustafson, T. Xiao, S. Whitehead, A. C. Berg, W.-Y. Lo, P. Dollár, and R. Girshick, "Segment anything," *arXiv:2304.02643*, 2023.
- [6] M. Teng, A. Ouaknine, E. Laliberté, Y. Bengio, D. Rolnick, and H. Larochelle, "Assessing sam for tree crown instance segmentation from drone imagery," 2025. [Online]. Available: <https://arxiv.org/abs/2503.20199>
- [7] A. Straker, S. Puliti, J. Breidenbach, C. Kleinn, G. Pearse, R. Astrup, and P. Magdon, "Instance segmentation of individual tree crowns with YOLOv5: A comparison of approaches using the ForInstance benchmark LiDAR dataset," *ISPRS Open Journal of Photogrammetry and Remote Sensing*, vol. 9, p. 100045, 2023. [Online]. Available: <https://www.sciencedirect.com/science/article/pii/S2667393223000169>
- [8] M. Teng, A. Ouaknine, E. Laliberté, Y. Bengio, D. Rolnick, and H. Larochelle, "Bringing sam to new heights: Leveraging elevation data for tree crown segmentation from drone imagery," 2025. [Online]. Available: <https://arxiv.org/abs/2506.04970>
- [9] S. Dersch, A. Schoettl, P. Krzystek, and M. Heurich, "Towards complete tree crown delineation by instance segmentation with mask r-cnn and detr using uav-based multispectral imagery and lidar data," *ISPRS Open Journal of Photogrammetry and Remote Sensing*, vol. 8, p. 100037, 2023.
- [10] H. He, F. Zhou, Y. Xia, M. Chen, and T. Chen, "Parallel fusion neural network considering local and global semantic information for citrus tree canopy segmentation," *IEEE Journal of Selected Topics in Applied Earth Observations and Remote Sensing*, vol. 17, pp. 1535–1549, 2024.
- [11] Y. Gui, W. Li, Y. Wang, X.-G. Xia, M. Marty, C. Ginzler, and Z. Wang, "Multimodal uncertainty robust tree cover segmentation for high-resolution remote sensing images," *IEEE Journal of Selected Topics in Applied Earth Observations and Remote Sensing*, vol. 19, pp. 114–128, 2026.
- [12] F. Hörst, M. Rempe, L. Heine, C. Seibold, J. Keyl, G. Baldini, S. Ugurel, J. Siveke, B. Grünwald, J. Egger *et al.*, "Cellvit: Vision transformers for precise cell segmentation and classification," *Medical Image Analysis*, vol. 94, p. 103143, 2024.
- [13] M. Pachitariu, M. Rariden, and C. Stringer, "Cellpose-SAM: superhuman generalization for cellular segmentation," *bioRxiv*, 2025. [Online]. Available: <https://www.biorxiv.org/content/early/2025/05/01/2025.04.28.651001>
- [14] J. Veitch-Michaelis, A. Cottam, D. Schweizer, E. N. Broadbent, D. Dao, C. Zhang, A. A. Zambrano, and S. Max, "Oam-tcd: a globally diverse dataset of high-resolution tree cover maps," in *Proceedings of the 38th International Conference on Neural Information Processing Systems*, ser. NIPS '24. Red Hook, NY, USA: Curran Associates Inc., 2024.
- [15] M. Weigert and U. Schmidt, "Nuclei instance segmentation and classification in histopathology images with stardist," in *The IEEE International Symposium on Biomedical Imaging Challenges (ISBIC)*, 2022.
- [16] F. Tong and Y. Zhang, "Individual tree crown delineation in high resolution aerial RGB imagery using StarDist-based model," *Remote Sensing of Environment*, vol. 319, p. 114618, 2025. [Online]. Available: <https://www.sciencedirect.com/science/article/pii/S0034425725000227>
- [17] B. Weinstein, S. Marconi, and E. White, "Data for the neontreeevaluation benchmark," Jan. 2022. [Online]. Available: <https://doi.org/10.5281/zenodo.5914554>
- [18] J. Troles, U. Schmid, W. Fan, and J. Tian, "Bamforests: Bamberg benchmark forest dataset of individual tree crowns in very-high-resolution uav images," *Remote Sensing*, vol. 16, no. 11, 2024. [Online]. Available: <https://www.mdpi.com/2072-4292/16/11/1935>
- [19] J. Lungo Vaschetti, E. Arnaudo, and C. Rossi, "TreePseCo: Scaling individual tree crown segmentation using large vision models," *The International Archives of the Photogrammetry, Remote Sensing and Spatial Information Sciences*, vol. XLVIII-M-7-2025, pp. 275–282, 2025. [Online]. Available: <https://isprs-archives.copernicus.org/articles/XLVIII-M-7-2025/275/2025/>
- [20] S. Ruschhaupt, J. Troles, and U. Schmid, "Comparing mask r-CNN and mask2former architectures for individual tree crown delineation," in *45. GIL-Jahrestagung, Digitale Infrastrukturen für eine nachhaltige Land-, Forst- und Ernährungswirtschaft*, 2025.
- [21] J. G. Ball, S. H. Hickman, T. D. Jackson, X. J. Koay, J. Hirst, W. Jay, M. Archer, M. Aubry-Kientz, G. Vincent, and D. A. Coomes, "Accurate delineation of individual tree crowns in tropical forests from aerial rgb imagery using mask r-cnn," *Remote Sensing in Ecology and Conservation*, vol. 9, no. 5, pp. 641–655, 2023.